Diode Array Camera Tubes and X-ray Imaging

By ARTHUR N. CHESTER, THOMAS C. LOOMIS, and M. M. WEISS

(Manuscript received September 11, 1968)

A modification of the silicon diode array camera tube has been carried out which permits X-ray images to be displayed on a television monitor. The silicon target, 50 to 150 μm thick, serves as the tube's vacuum window. Each X-ray photon generates a large number of holes in the silicon substrate. Most of these can be usefully collected, and effective quantum efficiencies over 1000 have been measured. Absolute measurements of the spectral sensitivity have been made and show good agreement with theoretical predictions made using values of hole lifetime and surface recombination velocity obtained from optical measurements on the same target. The silicon diode array offers a number of inherent advantages in X-ray imaging compared with the conventional amorphous selenium target. Among these are greater quantum efficiency, high sensitivity, and temperature stability. The diode array sensitivity greatly exceeds that of film in this X-ray energy range (5 to 20 keV). Moreover, because the video signal current is linear as a function of X-ray photon flux over a wide dynamic range, relative intensities may be compared directly rather than necessitating densitometer measurements as does film. The performance of the many types of X-ray imaging systems in different applications is compared in some detail.

I. INTRODUCTION

The silicon diode array camera tube, developed for *Picturephone*® visual telephone service applications,[1] has proved to be a versatile device. The possibility of using the diode array target for X-ray imaging had been discussed on various occasions, but a particularly useful step was the realization by E. I. Gordon that, since each X-ray photon could produce a great number of hole-electron pairs, very high quantum efficiency might be expected in this application.[2] Sub-

sequent measurements bore out this expectation.[3, 4] There are many uses for a practical imaging device with high visual brightness, ranging from medical and biological research applications to production-line testing of silicon wafer crystal orientation.[5]

This paper describes the modification of the camera tube for X-ray imaging and measurements of spectral response obtained with such a tube. The relevant features of all the various X-ray imaging techniques are compared in the context of specific applications to identify the particular devices which are most suitable for specific purposes. This permits a balanced evaluation of the usefulness of the silicon diode array camera tube for X-ray imaging, as well as shedding light upon other possible imaging systems.

II. DESCRIPTION OF DETECTION SYSTEM

The fundamental unit of the detection system is the diode array camera tube[1] developed for the *Picturephone* visual telephone station set. Let us start with a brief summary of the operation of this tube, as it applies to X-ray detection.

The camera tube target consists of a thin disk of n-type silicon, typically 0.800 inch in diameter, whose uniform thickness may range from 0.7 mil up to several mils, depending upon the specific application.

An array of p-n diodes is formed on one side of the silicon disk by standard photolithography and diffusion. Early versions of the target used diodes of 8-μm diameter spaced on 20-μm centers, covering a rectangular area approximately 1 cm on a side. In recent versions the diode spacing is 15 μm. These dimensions are consistent with specifications for the *Picturephone* visual telephone set and are not necessarily optimum for X-ray applications.

The target substrate is maintained at a potential of 5 to 10 volts positive relative to the electron gun cathode by the target bias voltage. An electron beam is scanned across the diode array, building up a negative charge on the p-side of the diodes until that surface of the target is charged down to cathode potential; then additional arriving electrons are repelled and do not land on the target (these are collected at another electrode, the collector). Under these conditions the diodes are reverse-biased, and in the absence of light will store their charge for a long time. The storage time is limited by diode leakage current. The amount of charge that leaks off between the successive times that the electron beam accesses a given diode (the frame time)

is replaced when the electron beam reaches that diode again. The associated charging current constitutes the video signal. The charging current observed when the target is not illuminated is called the dark current.

The detection ability of the diode array arises because the rate at which the diodes discharge can be greatly accelerated by various means. For *Picturephone* visual telephone service applications, an optical image is focused on the side of the silicon disk opposite the diodes. Photons create hole-electron pairs in the substrate; the holes diffuse to the nearest diodes and are swept across the space charge region, partially discharging the diodes. For X-ray detection, an X-ray photon is absorbed by a substrate atom, producing a fast electron carrying most of the original photon energy.[6] This electron creates many hole-electron pairs as it decelerates, losing its energy in a distance of no more than a few μm.[7] The resulting holes diffuse to adjacent diodes and discharge them. In either case, a video signal will be produced when the electron beam accesses those portions of the target which have been discharged by exposure to light or X-rays.

In the present work, the diode array was scanned in 275 horizontal lines; the frame time (the time required to scan all diodes once) was 1/30 second. The video bandwidth was about 1 MHz, and the picture was displayed on a TV monitor .

Provision was also made for blanking off the electron beam, allowing only every Nth frame to be read. This technique, described as "N:1 frame delay," allows the diodes longer between sweeps to lose charge in response to X-ray flux; thus within limits it increases the magnitude of the video signal obtained by increasing the integration time of the camera tube. This is simply analogous to using a longer exposure time in photographic work. The result is increased contrast in the displayed image.

The normal diode leakage current is also integrated; however, the extra dark current signal that results is not deleterious for storage times up to $\approx$1 sec. After a sufficiently long delay all diodes will discharge completely because of leakage, regardless of X-ray signal; thus excessive frame delay reduces picture contrast. The other undesirable feature of excessive frame delay is that moving objects will blur when frame delay is too long. In the early stages of the experiment, very long frame delays were subjectively unpleasant to use because the picture would only be displayed a few times a second, leading to flicker; however, this effect has now been minimized by using a long-persistence cathode-ray-tube in the monitor and could

be eliminated completely by using a storage tube for repetitive display of the same frame.

The diode array target is ordinarily mounted inside the camera tube vacuum envelope behind a glass window 0.100 inch thick. Since that thickness of glass would have introduced excessive attenuation of X-radiation, for X-ray use the tubes were assembled without mounting a diode array in the tube. The glass window of the tube was replaced with a copper plate in which a hole of ⅜ inch diameter was drilled. The diode array target was attached to the outside of the window, covering this hole, with Delta-Bond adhesive,* a high-temperature epoxy with clean vacuum characteristics. The tube was processed at a temperature of 190°C. Thus the diode array target itself served as the tube window and had to support the tube vacuum against atmospheric pressure. The target used in this work had a mechanically measured thickness ranging from 0.0104 to 0.0109 cm and a phosphorous diffusion at the back surface to reduce the hole recombination velocity at the surface. Because of dimpling in the target, resulting from the pressure difference, and the lack of beveling around the hole, causing distortion in the electric field between the last focusing element and the target, the electron beam could only provide uniform sensitivity over an area about ¼ inch in diameter on the target. Other tubes have now been constructed which avoid target distortion by using a beryllium or mylar window to hold the vacuum, allowing the target to be mounted inside the tube more or less conventionally. The usable sensitive area of the target in such tubes is the size of the entire diode array (1.34 × 1.34 cm in the present design).

III. CALIBRATION OF A MONOCHROMATIC HIGH-INTENSITY X-RAY SOURCE

A fluorescence X-ray tube with a copper anode was used to excite characteristic X-radiation from nine different samples, ranging in atomic number from vanadium to tellurium, as indicated in Table I. This radiation passed through a brass collimator 4 inches long with a 3/16 inch inside diameter, into which brass tubes of smaller inside diameter could be inserted to provide further collimation. The detector was positioned so that its window was 2.01 cm from the collimator. To reduce the energy spread of the resulting radiation an appropriate absorbing foil was introduced into the output beam, consisting of an element with a critical absorption energy just above the $K\alpha$ lines of

* Wakefield Engineering, Inc., Wakefield, Mass.

TABLE I—COMBINATIONS OF RADIATORS AND ABSORBING FOILS USED

Radiator			Foil			Representative Calculated Values of Photon Flux Using 40 mA Tube Current, Full Wave Rectification, with an Aperture of the Indicated Diameter		
	X-ray Fluorescence, keV							
Material	$K\alpha_1$	$K\alpha_2$	Thickness inches	Material	Absorption Edge, keV	0.020" photons/min	2.21 mm photons/sec	Peak Voltage kV
V	4.952	4.944	0.0016	Ti	4.964	456301	577139	40
Co	6.930	6.915	0.0028	Fe	7.111	314037	397200	40
Zn	8.638	8.615	0.0018	Cu	8.980	236438	299052	40
As	10.543	10.507	0.0042	Ge	11.103	157273	198922	40
Zr	15.774	15.690	0.0026	Y	17.037	419462	530544	40
Mo	17.478	17.373	0.0052	Zr	17.998	259854	328669	50
Pd	21.175	21.018	0.0057	Rh	23.224	87328	110454	50
Sn	25.270	25.042	0.0060	Ag	25.517	119537	151193	50
Te	27.471	27.200	0.0049	Sn	29.190	172146	217734	50

the radiator being used. It was determined by using a proportional counter with a multichannel pulse-height analyzer that the absorbing foil removed not only a great deal of X-radiation at lower energies, but also greatly attenuated the Kβ lines produced by the radiator. Thus the transmitted radiation was essentially monochromatic, consisting only of the Kα lines of the radiator being used, and ranged in energy from 4.95 keV (2.5 Å wavelength) to 27.3 keV (0.45 Å wavelength).

Once combinations of radiators and foils had been selected to provide X-radiation only in narrow spectral ranges, it was necessary to calibrate the absolute intensity of the output beam. This was done using a scintillation counter with a Siemens GS-DM ZO/B X-ray detector. By using a cobalt radiator with varying numbers of 0.003 inch aluminum absorbing foils, it was determined that this detection system reads 1 percent too low because of counter dead time loss at a count rate of 300,000 per minute; apertures were therefore chosen to keep all count rates on the Siemens detector below this level for the remainder of the measurements.

The detector used for calibration was a General Electric SPG 4 scintillation counter. The counting efficiencies used were calculated for a NaI crystal of nominal thickness 0.040 inch. Experiments are under way to establish an accurate experimental efficiency curve for this detector.[8] The efficiency of the Siemens detector was determined by comparison with the GE detector, using a crystal monochromator source, and was found to vary from 60.1 percent at vanadium to 88.6 percent at tellurium. The peak efficiency was 90.5 percent for cadmium Kα; the efficiency was above 79 percent for all the wavelengths subsequently used except the vanadium Kα.

Measurements were then made of the photons per second issuing from an aperture of diameter 0.020 inch for tube currents of 40, 11, and $\approx$2 mA, using a full-wave rectified power source, with peak tube voltages of 40 and 50 kV. Background intensities were subtracted in all cases. The statistical precision of these measurements was adequate to give a fractional standard deviation ($N^{-1/2}$) of 0.003 or less for each wavelength.[9]

In order to provide more X-ray intensity for detection by the silicon camera tube, a series of apertures of increasing size was used, finally arriving at an aperture 2.21 mm in diameter. The proportional counter was used to obtain intensity ratios between various apertures, and the final value for the intensity using the 2.21-mm aperture relative to that using the 0.020 inch aperture was determined to be 75.9,

with a calculated statistical precision of 3.5 percent. The maximum calibrated intensity available varied from 110,000 to 577,000 photons per second, depending upon the X-ray energy, as indicated in Table I.

The particular combination of aperture, radiators, foil filters, detector distance, and X-ray source measured thus provides a variable-energy monochromatic output of known intensity. If the instability of the power supply-detector combination is taken to be 0.2 percent, this indicates that the relative intensities available at different energies are known with a standard deviation of 0.36 percent, and the absolute intensity at any given wavelength is known with a standard deviation of 3.5 percent.

IV. MEASURED X-RAY SPECTRAL RESPONSE AND SENSITIVITY

The camera tube was mounted with its diode array target 2.01 cm from the 2.21-mm aperture and the X-ray beam was chopped at 13 cps using a lead chopper blade. The video signal was synchronously detected to provide greater measurement accuracy. It was verified that the video signal obtained did not change when the size of the scanned area on the diode array was increased. The magnitude of the 13-cps signal was compared with the video signal measured with a dc meter without chopping the X-ray beam; the rms deviation in this calibration factor was found to be 3.8 percent. This introduces an error in the absolute scale of the measurements, in addition to the 3.5 percent resulting from errors in measuring intensity ratios using different apertures.

The noise in the synchronous detector signal had an rms value of 0.2 microvolts. An X-ray beam whose intensity was just sufficient to give a signal on the synchronous detector equal to this noise level, if directed onto the camera tube without chopping, would have given a dc video current of 0.79 pA. Since video currents of about a nanoampere were required to produce a strong image on the monitor with the beam size used here, many of the X-ray intensities measured therefore did not produce a visible spot on the monitor. The error bars indicated in the graphs indicate the range of values represented by this error of 0.2 microvolts, since the 0.36 percent error in the relative calibration of the X-ray source was too small to affect the accuracy of these measurements. The overall presumed accuracy of $[(3.5)^2 + (3.8)^2]^{1/2} = 5.2$ percent is not indicated in the figures but should apply to the absolute magnitude of the measurements.

Figure 1 indicates the dc response of the diode array camera tube

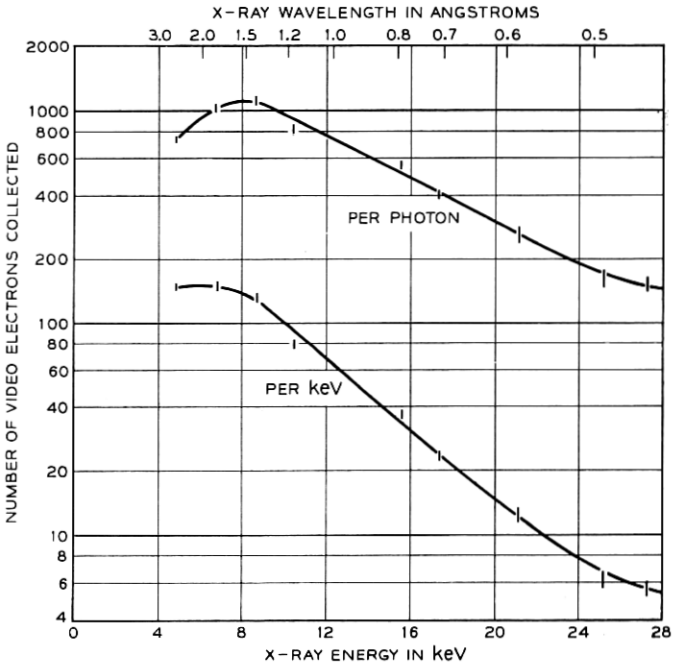

Fig. 1 — Video electrons collected by tube No. TN-84 as a function of incident X-ray energy.

as deduced from the synchronous detector measurements. Since the number of hole-electron pairs produced when an X-ray photon is absorbed is a linear function of the available photon energy, it was felt that it was most meaningful to plot numbers of collected electrons as a function of photon energy rather than photon wavelength. Figure 1 gives the number of video electrons collected per incident X-ray photon and per keV of incident X-ray photon energy.

V. DETERMINATION OF TARGET SUBSTRATE PARAMETERS

In order to extract information more indicative of the physical processes leading to the X-ray detection, some further processing of this data is necessary. If information can be extracted about the intrinsic quantum efficiency of the detection process, then the practical performance of diode array targets of various thicknesses and various physical properties can be estimated. In this section the hole lifetime and surface recombination velocity are determined for the target used in our experiments.

One piece of information necessary for this computation is the absorption coefficient of the diode array target for the various wavelengths of X-rays used. This information is well known, and for this work was taken from a table published by Philips Electronic Instruments.[10]

It is also necessary to know the distribution in position of the holes generated in the silicon when an X-ray photon is absorbed. This is relatively simple to determine under the assumption that the X-ray photon upon absorption produces a very fast electron carrying most of the photon's energy; this electron then produces many hole-electron pairs as it loses energy. The rate of production of the fast electrons decreases exponentially with distance as the X-ray beam is absorbed; thus the rate of hole production will also have this exponential profile, spread out slightly by the range of the fast electrons in the silicon substrate. However, an estimate of the range of fast electrons of the appropriate energy yields values less than 5 percent of the 1/e absorption distance for X-rays in silicon in the energy range treated here. Thus a hole production rate that decays exponentially with distance will be assumed in this energy range.

The last piece of information that is needed is the fraction of holes generated that are collected by the diode and thus lead to a video signal, for the exponentially decaying hole generation rate previously obtained. This can be determined fairly well as follows. The absorption mechanism for photons in the near infrared is primarily hole-electron pair formation, the photon energy involved being sufficiently small that only one hole can be produced per photon absorbed. Moreover, different hole generation geometries can be obtained since the absorption coefficient of the silicon varies as a function of wavelength. To duplicate the X-ray absorption depths relevant to the measurements reported here, it would be necessary to use infrared light varying in wavelength from 0.87 to 1.11 microns.[11]

However, even though light and X-radiation are chosen having the same absorption depth in silicon, the hole generation geometry may differ in the two cases. Unless the absorption coefficient is sufficiently great that virtually all of the light is absorbed in a single pass through the target substrate, light will be reflected from the surface at which the diodes are located, changing the simple exponential spatial dependence of the hole generation rate to some more complicated form, and making the hole generation geometry different for the light and the X-rays. Since absorption and optical interference are known to take place[12] in the oxide-resistive overlay region, even

the reflectivity of the diode surface of the substrate is complicated and wavelength-dependent.

Crowell and Labuda have developed a recombination-diffusion model for hole collection in a diode array target which is valid for light in the visible part of the spectrum, where multiple internal reflections may be ignored.[13] The measured optical collection efficiency of the diode array target in this wavelength range can be used to determine sufficiently accurately the two parameters required in this model, namely, the hole lifetime in the substrate and the hole recombination velocity at the illuminated side of the target. Although the collection efficiency predicted by the model becomes invalid when applied to infrared light, it is perfectly valid for X-rays of all wavelengths, since X-radiation maintains the exponential hole generation geometry regardless of the absorption of the substrate because the X-rays are not appreciably reflected at the surfaces of the silicon. Crowell and Labuda's collection efficiency model was applied to the X-ray camera tube to determine the necessary target parameters.

First, measurements were made of the number of video electrons collected per incident photon for light in the wavelength range 0.46 to 1.15 microns. Since A. J. Chick's computer calculations of the collection efficiency predicted by Crowell and Labuda's theory did not include the effects of reflection at the silicon-air interface and the "dead layer"[14, 15] at the illuminated side of the silicon target, the measured collection efficiency was corrected before comparing with the theoretical curves.

The measured collection efficiency was first multiplied by a factor, $\exp(+\alpha L_d)$, to eliminate effects resulting from absorption in a "dead layer" of thickness $L_d = 0.2$ μm. The absorption coefficient α of silicon for visible light was taken from published data.[11] The measured collection efficiency was further increased by $1/(1 - R)$ to correct for reflection at the silicon surface, using published values of the reflectivity of silicon.[16] This yielded the open data points shown in Fig. 2, which represent as accurately as possible the number of video electrons collected per optical photon passing through the dead layer into the active region of the substrate.

The reflectivity of the diode array was measured, as described in the Appendix, to verify that the reflectivity corrections being made were accurate. If the measured values of reflectivity are used to obtain the collection efficiency for wavelengths greater than 1 μm in Fig. 2, the two solid data points are obtained. However, Crowell and Labuda's theory neglects internal reflections. Thus the corrected values of col-

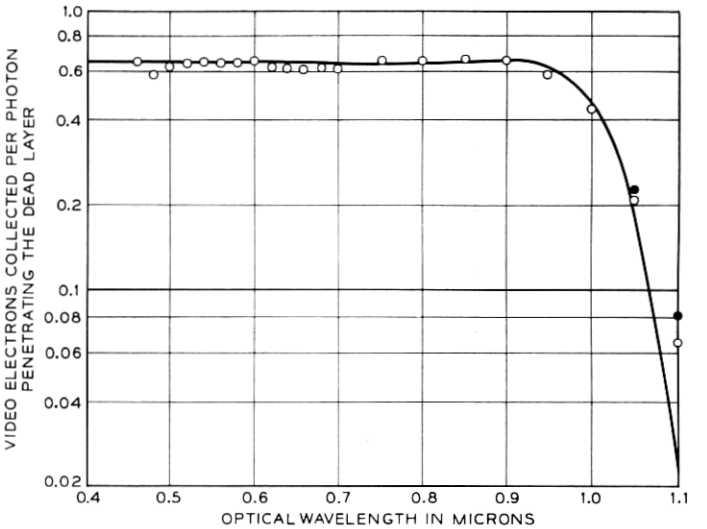

Fig. 2 — The data points represent measured values of collection efficiency for tube No. TN-84, corrected for reflectivity and dead layer absorption as discussed in the text. The solid data points use measured values of reflectivity rather than published values. The solid curve gives the predictions of Labuda's theory, which is expected to be valid only at wavelengths shorter than $\approx 0.93 \mu m$ because of its neglect of internal reflections.

lection efficiency shown in Fig. 2 may be used only at sufficiently short wavelengths such that the exponential hole profile within the substrate caused by the incident photons is not distorted by internal reflection from the diode surface of the target. To keep the intensity of light arriving at the diodes below 5 percent of that entering the target, the target thickness must be about three times the $1/e$ absorption depth. In the present target, with thickness of about 0.0107 cm, this requires considering in Fig. 2 only those wavelengths shorter than ≈ 0.93 μm.

The predictions of Crowell and Labuda's theory were then calculated for various values of hole lifetime τ and surface recombination velocity S. The depletion layer depth was taken to be 5 μm, a typical value for the conditions of vidicon operation (substrate resistivity 10 ohm-cm, target voltage 5–10 volts).[17] The theoretical predictions were compared with the experimental data as follows.

Computed collection efficiency curves were drawn for a large number of values of S, ranging from 50 to 1000 cm per second, with τ ranging from 5 μsec to 10 msec. These ranges of values were known from previous work to include any values of the parameters which

might be encountered. The values of the collection efficiency at 0.50 μm wavelength and at its maximum were found to give good discrimination between the curves, and the values of S(cm/sec), τ(μsec) selected for further comparison were: (50, 11), (70, 12), (100, 12), (100, 13), (140, 13), and (140, 14). The rms deviations of these curves from the measured values (with oscillatory behavior removed as discussed in the Appendix) were calculated for wavelengths 0.50, 0.65, 0.80, and 0.90 μm, and the maximum value. Only one curve was found to agree within one averaged deviation at as many as four of these points; moreover, at the remaining point it was still only 1.35 averaged derivations away from the measured value.

The values determined by selecting this curve as the best fit were $\tau = 12(\pm 0.5)$ μsec and $S = 70(-10, +15)$ cm per second. This is shown as the solid curve in Fig. 2. The uncertainties quoted assume a probable error of half the interval to the next closest values of S or τ examined. These values are consistent with the values $\tau = 10$ μsec, $S \approx 50$ cm per second found by Buck, Casey, Dalton, and Yamin in similar diode array targets.[14] The hole diffusion coefficient D in silicon has been taken as 10 cm^2 per second[18].

VI. CALCULATED SPECTRAL RESPONSE OF DIODE ARRAY TARGETS

Using the values determined above for the hole lifetime and surface recombination velocity, a predicted X-ray quantum efficiency may be calculated for comparison with the measured values in Fig. 1. This is done for a variety of target thicknesses to provide an estimate of how the collection efficiency would be expected to change with target thickness, since it would be desirable for many applications to extend the spectral response to higher X-ray photon energies.

First, an upper limit to the number of video electrons collected per incident photon may be calculated, which will ultimately limit the performance of any silicon diode array target which does not incorporate heavier elements in substantial quantities. This is obtained by assuming that the holes produced by every X-ray quantum absorbed in the target are all collected, so that the limitation on quantum efficiency at low energies is the smaller energy per photon available for making hole-electron pairs, and at higher energies is the lack of absorption of these X-ray photons by silicon. Specifically, the fraction of X-ray photons absorbed by the target is obtained using published X-ray absorption coefficients for silicon.[10] It is then assumed that each 3.50 eV of energy in an absorbed photon leads

to a video electron. Such a calculation is consistent with a model which assumes that virtually all of the photon energy is transferred to an electron upon absorption; this fast electron produces hole-electron pairs as it decelerates (expending for each pair the value 3.50 eV),[19] all of the resulting holes are collected.

Such a calculation leads to the collection efficiency curves in Fig. 3, which give an upper limit to the quantum efficiency that could be anticipated using any target principally composed of silicon. The rise in collection efficiency in the 100 keV range occurs because the absorption coefficient of silicon, which drops approximately as E^{-3}

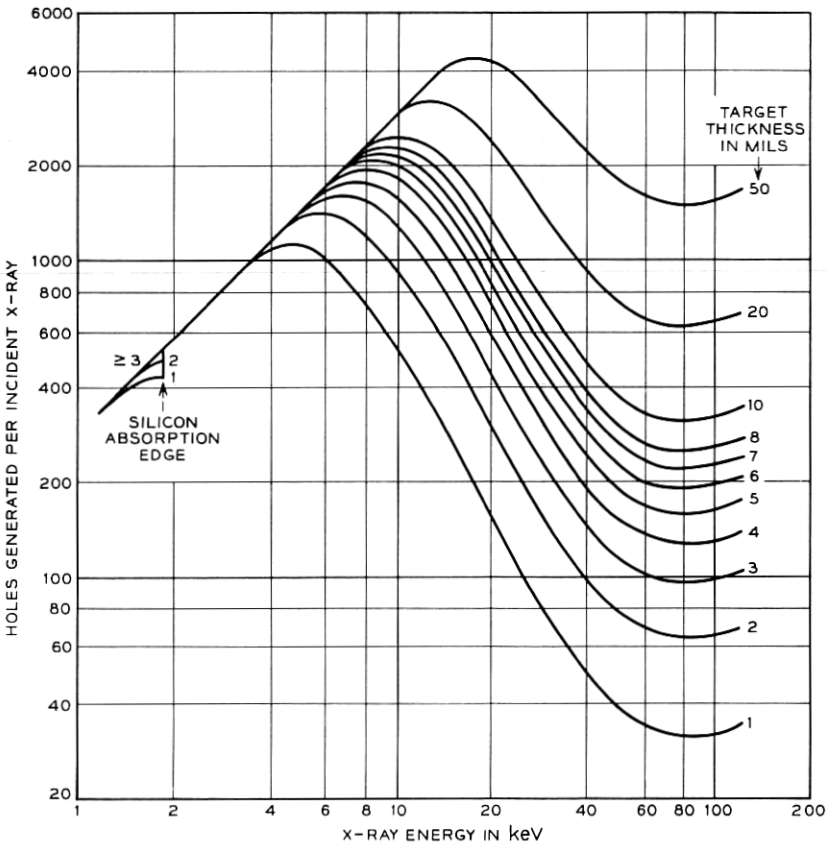

Fig. 3 — Maximum number of holes that could be generated per X-ray photon incident upon silicon targets having the indicated thickness, as a function of X-ray energy.

for X-ray energies in the range 2 to 30 keV, drops less rapidly at higher energies, falling at a rate slower than $1/E$ above 85 keV. This slower drop is more than compensated for by the greater energy available per photon which, of course, rises linearly with E. However, since this increased absorption occurs from Compton scattering rather than the photoelectric effect,[6] it may be less efficient at producing hole-electron pairs.

The additional information, provided by the values $\tau = 12$ μsec and $S = 70$ cm per second obtained in the previous section, permit more specific calculations to be made for the conventional type of diode array target having a "dead layer" of thickness 0.2 μm, with holes generated in the substrate either diffusing to a diode and being collected, recombining in the volume, or diffusing to the illuminated side of the target and recombining with electrons without leading to a video signal. The depletion layer thickness will again be assumed to be 5 μm.

The calculation is made using Crowell and Labuba's collection efficiency theory, corrected for the presence of the dead layer, again assuming that every 3.50 eV of absorbed X-ray energy leads to the production of a hole. A computer program by A. J. Chick using this theory leads to the curves in Fig. 4, which predicts the actual X-ray collection efficiency that should be observed using silicon diode array targets of various thicknesses, with the substrate parameters taken to be $\tau = 12$ μsec, $S = 70$ cm per second.

Notice that the target thickness yielding the greatest collection efficiency is about one hole diffusion length L_D in thickness, since $L_D = (D\tau)^{\frac{1}{2}} \approx 4$ mils. The experimental points indicated in Fig. 4 for tube No. TN-84, with target thickness 4 mils, are $\approx$20 percent lower than the calculated values. This discrepancy may arise from error in estimating the dead layer thickness, lack of accurate experimental calibration of the X-ray source, and neglect of excess recombination[20] in the theoretical treatment. Other contributing factors may be electrons lost by photoemission at either surface of the target and a ± 5 percent uncertainty in the mechanical measurement of the target thickness.

One final curve of some interest is the quotient of the theoretical predictions of Figs. 4 and 3. Since Fig. 3 gives essentially the total number of holes generated per incident photon and Fig. 4 gives the number of electrons collected per incident photon, the quotient of these values is the fraction of generated holes which are usefully collected by the diodes. This number, referred to here as the "geometrical efficiency" of the target, depends only upon the geometry of

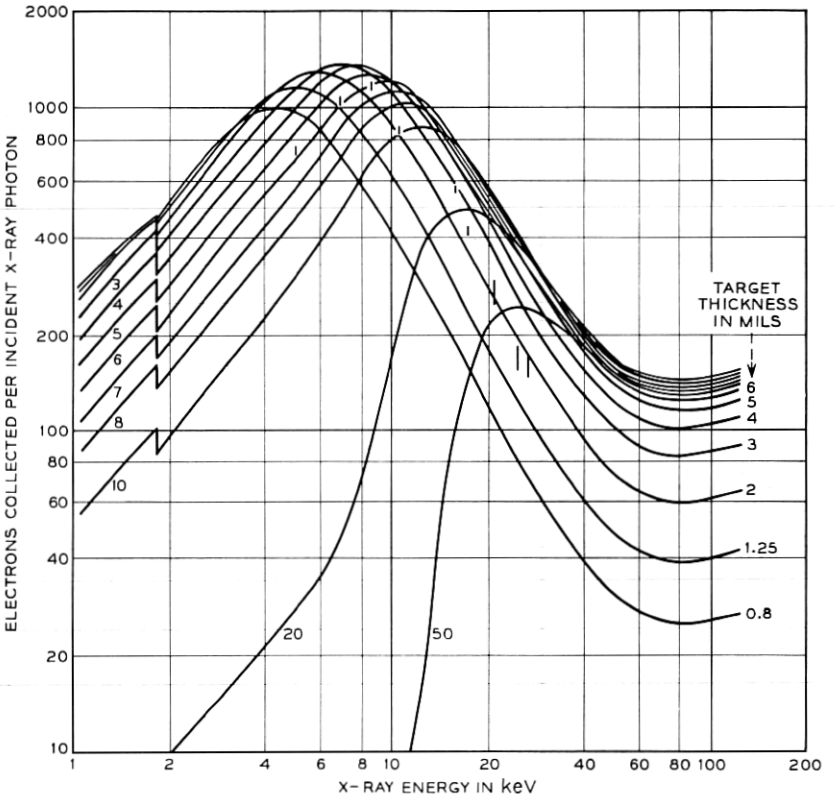

Fig. 4 — Collection efficiency for X rays as a function of X-ray energy, predicted by theory. Values measured for tube No. TN-84 are indicated.

the collection: absorption coefficient, substrate parameters, and target geometry. It is shown in Fig. 5 as a function of absorption coefficient, and the values presented apply to both X-ray detection and visible light detection, so long as the exponential hole generation geometry is maintained. Corresponding X-ray energies and optical wavelengths are indicated in the figure. As expected, the geometrical efficiency asymptotes to its maximum value when the absorption coefficient becomes so small that the hole generation is essentially uniform throughout the target volume.

VII. COMPARATIVE EVALUATION OF VARIOUS X-RAY IMAGING TECHNIQUES

The X-ray imaging devices known to the authors may be classified into the following categories:

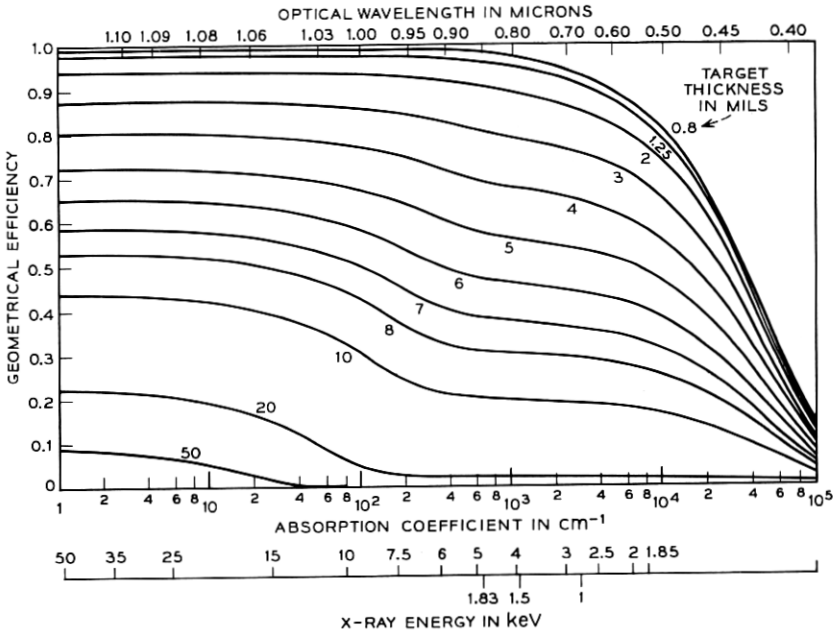

Fig. 5 — Geometrical efficiency of silicon targets of various thicknesses for visible light and X-radiation, assuming a dead layer of 0.2μm and strictly exponential hole generation.

(*i*) Film—Film may be directly sensitive to X-radiation or make use of a phosphor screen placed in close contact with the film.

(*ii*) Direct fluoroscopy—A fluorescent screen is viewed directly by a dark-adapted observer.

(*iii*) Image-intensified fluoroscopy—Systems in this category seem to have the common feature that image amplification occurs without dissecting the image sequentially. A conventional technique of this type uses a fluorescent screen in intimate contact with a photoemitter, taking the emitted electrons by electron focusing and minification to produce a brighter image on a cathodoluminiscent phosphor screen, which in turn may be viewed directly or imaged with a television system first. In this category would fall direct photoemission by X-rays, with later electron imaging. Another modification would replace the electron imaging stage by a solid-state image intensifier.

(*iv*) Flying spot tubes—A collimated X-ray beam is periodically scanned across an object to be examined, and a detector of high counting efficiency collects essentially all photons penetrating the

object. Although this is strictly speaking not an imaging system, it serves the same function for certain applications (for example, medical and radiographic) and therefore is to be considered competitive for such applications.

(*v*) Scanned-image camera tubes—These systems use sequential image dissection with subsequent electronic amplification. The tubes that have been constructed of this type use an electron beam to scan a photosensitive surface, usually a photoconductor. The diode array camera tube is in this category.

Qualitative comparisons among some of these systems have been given in the past.[21-30] The present discussion will be more quantitative and relate to specific practical applications.

7.1 *Microscopy*

The resolution element d is defined so that the modulation transfer function of the system is 50 percent at a spatial frequency of $1/2d$ line pairs per unit distance. The resolution obtainable with standard X-ray film is about a μm,[31, 32] and films of finer grain are available. Although film does not permit real-time viewing, it is still the most convenient choice for many applications, and can be used for motion studies by using a movie camera or a rotating film drum. The resolution of fluoroscopic screens ranges from 0.4 to 0.7 mm;[22, 29, 33-35] these are inappropriate for very fine imaging.

In scanned-image camera tubes a practical limitation likely to be encountered is bandwidth and electron beam spot size. Bandwidth is not too severe a limitation upon resolution, since it only limits the number of resolution elements in the picture (for a fixed frame time) rather than their size. Thus, finer detail may be observed at the sacrifice of viewing a smaller area of the image.

The limitation on electron beam spot size is more basic but again tradeoffs can be made. From Pierce,[36] the current density at a picture element, assuming an ideal lens, is

$$j_{\text{spot}} = j_{\text{cathode}}(1 + \Phi) \sin^2 \theta. \tag{1}$$

In this equation,

$$\Phi = eV/kT, \tag{2}$$

with V the target potential with respect to the cathode and T the cathode temperature. θ is the maximum angle with respect to the target normal which the paths of arriving electrons make, and j_{cathode} is the

emission current density at the cathode. For an approximate calculation one may take $V \approx 1$ volt, and $kT/e \approx 0.1$ volt, so that $1 + \Phi \approx 10$. In practical devices an appropriate value is $\sin \theta = 0.1$. The current density available from a CPC cathode (a typical choice for diode array camera tubes) as measured by MacNair is $j_{\text{cathode}} = 2.5$ A/cm^2;[37] this cannot be bettered by more than about a factor of four, and then only at the expnse of operating lifetime.[37] Thus a practical limitation is

$$j_{\text{spot}} = i_{\max}/d^2 \approx 0.25 \text{ A/cm}^2. \tag{3}$$

For example, in tubes now available the maximum beam current is about $i_{\max} = 6$ μA, giving a minimum spot size of $d \approx 50$ μm, which agrees approximately with experience.[38]

In an electron beam scanned device, therefore, a spot size $d = 5$ μm, according to these considerations, permits only the relatively small amount of beam current $i_{\max} = 60$ nA; because of secondary electron emission, the maximum signal current available is still less. Practical difficulties in design, because of nonideal imaging, may make such small spot sizes hard to achieve. Thus, dynamic range must be sacrificed to get very high resolution with such a device.

The problem of lateral diffusion of carriers is particularly troublesome in connection with high resolution camera tubes. In the case of a diode array device there is virtually no electric field in the target substrate and carriers simply diffuse to the diodes. For an $S = 0$ surface[13] and lower energy X-rays, with the carriers generated near the surface, the carriers will, on the average, diffuse laterally a distance equal to the thickness t of the target while they diffuse an equal distance t to the depletion region of the diode. This lateral spread would give a picture element of approximate size $d = 2t$. This will only be slightly reduced (to perhaps $1.5t$) for X-rays of higher energy, even when a finite surface recombination velocity is taken into account. Since the minimum thickness for a self-supported target is about 10 μm at present, the attainable resolution for such a target is only about 15-20 μm. Higher resolution would probably suggest a thinner target, mounted on a beryllium entrance window. Similar considerations apply to other possible target materials, such as amorphous selenium,* PbO, or CdS (See Refs. 39 and 40, 21 and 41, and 21, respectively). However, these latter materials are not generally fabricated to be self-supported as is the diode array target.

Another effect that can be of some importance in determining the

* Westinghouse Type WX-5129 X-Ray Vidicon, Westinghouse Electric Corporation, Electronic Tube Division, Elmira, N. Y.

resolution arises from the nature of the primary photoprocess. Since a single fast photoelectron is produced when an X-ray quantum is absorbed, and since the velocity of that electron may have any direction with respect to the direction of photon incidence, the finite range of that electron's energy loss means that carriers are produced approximately throughout a sphere whose radius is the range of the hot electron in the substrate. The resolution element d will be taken to the diameter of that sphere. For example, in silicon an approximate value is[7]

$$d = 0.028[E(\text{keV})]^{1.65}\ \mu\text{m}. \tag{4}$$

This formula is quoted as having validity in the range 2 to 20 keV.[7] Since a similar formula given for the range of electrons in aluminum (only one less in atomic number than silicon) yields a value for range of 32.3 μm at 100 keV, not too far different from the measured value $\approx$55 μm,[42] it is reasonable to expect that the expression for silicon also retains validity to higher energies than 20 keV. This would indicate, in the case of silicon, a picture element of size d = 3.9 μm at 20 keV, increasing to 23.8 μm at 60 keV. The range for electrons would be expected to be smaller[42] for heavier target materials such as selenium, CdS, or PbO.

Finally, it is also possible that such effects as generation of secondary X-radiation and Compton scattering could impair resolution, especially at energies above 50 keV; these might have to be considered in the design of a very high-resolution camera tube.

The X-ray camera tube in its present form has an estimated resolution of about 25 μm. Depending upon the energy and intensity of the X-rays to be detected, the foregoing discussion indicates that this probably cannot be reduced to less than 5 or 10 μm in a camera tube of this type.

7.2 *Medical Applications*

For medical imaging applications it is desirable to have a large sensitive area (at least 6″, preferably 12″ in diameter)[34, 43, 44] and good video response to high energy X-rays, a typical effective X-ray energy being 60 keV. The former constraint does not apply to dental work. In addition, it is particularly necessary to minimize the dose to the patient by making effective use of as many incident X-ray photons as possible.

Film meets all these requirements most effectively when only a single picture needs to be made and when development time is not a

consideration. However, it is not practical for motion studies because of the inconvenience of sequentially exposing such large areas on successive frames of film.

Although direct fluoroscopy is very efficient in producing an optical image from the incident X-radiation, the eye is an inefficient gatherer of light and thus loses much of the advantage gained by the high quantum efficiency of the fluorescent screen.[22-24] Although the fraction f of usefully absorbed photons may be as high as 0.65, so that the majority of the incident X-ray photons are effective in producing visible quanta, each incident X-ray photon leads only to $\leqq 10^{-3}$ optical photons at the retina of the eye, so the effective f of the system must be taken to be this much smaller value.[22,24] Since this fraction f determines the amount of information transmitted by the detected photons, as pointed out by Rose,[45] for an f of 10^{-3} the statistical fluctuations in the detected signal are so great that only one-thousandth of the information contained in the incident photon flux is transmitted through the detection system.

When an image intensifier is used, the number of quanta per picture element never falls below the number originally usefully absorbed; the various stages of transmitting the picture information in the image intensifier system only act to increase the number of quanta per picture element, and even with the inefficiency of the eye's optics the number of photons reaching the retina is typically still an order of magnitude higher than the number of X-ray photons usefully absorbed.[22] Values of f for an image intensifier system could be as high as ≈ 0.65, depending upon X-ray photon energy, since the primary photoprocess uses this fraction of incident photons in direct fluoroscopy. However, in practice, thinner fluorescent screens are used in order to improve the resolving power of the system. Depending upon the energy of X-rays and the resolution required, values of f from 0.01 to 0.55 (but usually below 0.1) have been reported in these systems.[22, 24, 29, 46, 47] A useful compromise providing better resolution than direct fluoroscopy but still having a much higher effective f might be estimated to have $f = 0.1$.

Notice that with $f = 0.1$ only one photon in ten is detected. Thus even though the image intensifier display exhibits genuine quantum noise, it should be possible to reduce the dose to the patient a factor of ten without impairing the picture quality.

In addition to the present work, the usefulness of the silicon diode array camera tube for detecting X-rays in this energy range ($\approx$60 keV) has been demonstrated by Harpster and Jacoby.[48] To compute the

efficiency of the silicon tube and other photoconductive camera tubes (using PbO, CdS, and Se targets), it is first necessary to discuss some aspects of camera tubes using photoconducting targets. It has been shown, for example by Rose[49,50] and by Redington,[51] that the requirements of short response time (low "lag"), low dark current, and high photoconductive gain (referred to here as the geometrical efficiency g) cannot be simultaneously satisfied using ohmic contacts. The only way to keep g fairly large consistently with the other requirements is to use "blocking" contacts. Since these do not inject additional carriers from the electrodes the dark current can thus be kept acceptably low.

When a blocking contact is used, there is a depletion region adjacent to the contact, across which appears the voltage drop which is applied to the target. Carriers generated in this region are efficiently collected because of the electric field present, but carriers generated outside this region must diffuse to the depletion region before recombining if they are to be collected. Although the width of the depletion region can be widened by increasing the target voltage, in practice it is not generally possible to extend the depletion region throughout the target thickness because carrier injection will occur at higher voltages. This carrier injection increases dark current, and makes the contact effectively ohmic rather than blocking. Thus, although contacts to amorphous selenium X-ray vidicon targets are blocking in nature, the width of the depletion region is sufficiently small that most carriers are collected by diffusion rather than by being swept through a region by an electric field. This would explain why the optimum target thickness reported by Smith[40] was approximately equal to the carrier diffusion length, and is also consistent with depletion layer thicknesses discussed by Rose[49] and van den Broek.[52]

Since blocking contacts have been achieved in PbO,[52] amorphous selenium,[49] and CdS,[53] it is certainly possible to construct X-ray camera tubes, using such target materials, in which carriers are collected by diffusion to the electrodes, although the fabrication of the contacts may give some practical difficulty. Therefore such camera tubes can be easily compared with the silicon diode array tube since the method of carrier collection is similar and the same restraints that apply to the silicon tube (limited target thickness to prevent lateral diffusion of carriers and consequent resolution loss, and to prevent loss of carriers by volume recombination before collection) will also apply to these tubes.

If blocking contacts can be maintained at sufficiently high voltages that the depletion region can be extended through the target thick-

ness, the sensitivity will be much greater than estimated here. Such contacts were apparently not obtained in the work reported by Smith on amorphous selenium targets.[40] In the case of PbO films, the authors are not aware of X-ray measurements reported in sufficient detail to determine the mechanism of carrier collection.

The applicability of various camera tube targets to medical X-ray detection can be assessed under the assumption that the generated carriers diffuse to the target surface and are collected there. The targets will be assumed to be as thick as possible so that as much of the incident radiation as possible can be used. Specifically, the target thickness will be taken to be ten times the diffusion length for minority carriers in the particular substrate being considered. This is as thick as can be allowed if each absorbed photon is to produce at least several collectable carriers, since $e^{-10} \approx 10^{-4}$ and since a 60 keV photon produces around 10^4 carriers in each of these materials. In any case, this manner of choosing the thickness is sufficiently general to provide some sort of meaningful comparison, particularly since the geometrical efficiency g should be similar for all four types of targets, as discussed in connection with Table III. A comparison of these types of camera tubes appears in Table II.

According to results obtained in Section 7.1, the resolution of such camera tubes would be expected to be better than the 0.4 mm obtainable with fluorescent screens, since such screens are subject to lateral

TABLE II — COMPARISON OF CAMERA TUBES FOR MEDICAL APPLICATIONS

Substrate Material	Diffusion Length μm	Target Thickness μm	X-ray Photon Energy			
			40 keV		60 keV	
			α, μm^{-1}	f	α, μm^{-1}	f
PbO (tetragonal)	1.2*	12	0.0132†	0.147	0.00492†	0.0573
Se (amorphous)	10‡	100	0.00365§	0.306	0.00115§	0.109
CdS (n-type)	6.4¶	64	0.00703†	0.362	0.00256†	0.151
Si (n-type)	110||	1100	0.000176§	0.176	0.00008§	0.084

* See Ref. 56.
† See Ref. 57.
‡ See Ref. 40, p. 352.
§ See Ref. 10.
¶ Reported values differ by about a factor of two, but the value given here is typical. It is obtained from the equation $L = (D\tau)^{1/2}$ using a hole diffusion constant $D = 0.27$ cm²/sec and hole lifetime $\tau = 1.5$ μsec. These values are given by I. Broser, *Physics and Chemistry of II-VI Compounds*, ed. M. Aven and J. S. Prener, New York: John Wiley and Sons—Interscience, 1967, p. 520.
|| Calculated from measurements reported in Fig. 2 of this paper.

light scattering. The values of absorption coefficient α for X-rays, as indicated, are given in inverse μm. The fraction of photons usefully detected is taken to be simply $f = 1 - \exp(-\alpha t)$ for thickness t.

The table indicates that only using CdS in a scanned image tube offers hope of improvement in usable fraction f over conventional optical image-intensifier systems as long as carrier collection depends upon diffusion. Its combination of high density and ease of fabrication makes it a possible candidate for medical applications. A silicon target has not only the disadvantage of a lower f, but the problems connected with a higher dark current, as discussed in the following section.

However, the very best imaging device for medical applications remains the final possibility considered here, the flying spot X-ray system. Although the production of X-radiation by such a system is necessarily very inefficient, about 90 percent of the photons transmitted by the patient can be detected with certainty, and thus this system is to be preferred if cutting the dose to the patient is the principal consideration. However, the practical difficulties of producing sufficient X-ray intensity in a scanned X-ray beam seem to still remain an essential limitation to the method. Discussions of this system appear in Refs. 23, 27, and 54.

7.3 *X-Ray Diffraction and Other Applications*

The type of application toward which this section is oriented is the case of an X-ray image of limited intensity which is to be detected as conveniently as possible. A typical application in mind here is that of Laue diffraction work. Another, usually applicable to higher energy X-radiation, is industrial radiography.

As in the case of many other applications, film is useful but not always the optimum detector. Its variable exposure time gives it effectively a very wide dynamic range, but it is highly nonlinear (gamma $\neq 1$)[55] and relative intensities cannot be easily measured.[28] The desire to see a picture more rapidly, either by reducing exposure time or eliminating the developing process, or both, provides motivation to consider other imaging systems. Moreover, the increased sensitivity provided by alternate systems for low energy X-radiation may permit imaging in cases where the required film exposure time would lead to excessive fogging.

Image intensifier systems have been used in the past in such applications as Laue diffraction work, to allow continuous monitoring of the diffraction pattern as a crystal is oriented.[23,35,47] The inherent limita-

tion in these systems is their limited resolution of $d \approx 0.4$ mm, owing in part to lateral scattering of light.[22]

Scanned-image tubes can improve upon resolution, permitting orientation of very small crystals (requiring more highly collimated beams) or more accurate measurement of larger crystals than would be possible with an image intensifier system. Because of unity gamma, relative intensities at a given X-ray energy may be measured electronically. In addition, the integration time during which the image is being accumulated in the charge pattern on the target can be varied electronically, corresponding to varying the exposure time when using film.

There are several ways in which scanned-image camera tubes may be compared. The points of comparison are charge storage time, sensitivity, and convenience. Since, in a tube without electron multiplication, amplifier noise usually dominates, comparison of sensitivity also constitutes an evaluation of signal-to-noise ratio or picture quality.

The difference between the applications currently under discussion and medical applications is that rather than there being a limitation upon total number of photons incident upon the viewed object, there is instead a limitation upon the total photon flux rate available to illuminate it. Thus the number of incident photons per picture element is proportional to the integration time τ_i which is used to accumulate the picture. Since the signal increases linearly with τ_i but the noise increases no faster than the square root of τ_i, it is advantageous to use the longest integration time that is consistent with linear system response and operator convenience. If changes in the image are to be observed, for example changes in a Laue pattern as a crystal is oriented, it is probably desirable that the integration time not exceed $\approx$1 second, and frequently preferable to make it even less, say 0.1 second.

Since the integration time may be arbitrarily increased without changing frame time by frame delay, as described in Section II, the maximum integration time that can be used is determined simply by the duration of time for which charge can be stored on a picture element. In the case of a photoconducting camera tube this time constant can be very long. Charge storage times longer than 2 minutes have been reported for tubes with amorphous selenium targets,[40] and similarly long storage times should apply to photoconductors with such high dark resistivities as PbO[56] and CdS.

In a diode array target, the dark leakage current determines the charge storage time. For tube No. TN-84, it was found that the dark

current was a linear function of the quantity (V_T — 1.5 volts) over the range $1.5 \leqq V_T < 5$ volts. It will be assumed that an appropriate model for the effect of the dark current is therefore a resistance R connected across the diode capacitance C. Because of the nature of the photo-process, absorbed photons may be represented by a current generator. The electron beam is represented by a battery of voltage $V = V_T - 1.5$ and a switch whose momentary closure represents the scan of the electron beam across the diode in question. The current through the battery is the video current. This extremely simple equivalent circuit is shown in Fig. 6.

Consider the following experiment: The electron beam is blanked off at $t = 0$, just after reading a frame, and after a time τ a source of optical or X-ray photons is flashed briefly on. This source is confined to a limited area of the target so that both light and dark signals are available for comparison. Now after an additional time T during which there is no photon source and still no electron beam, the electron beam is again turned on and allowed to scan. As the electron beam sweeps the target, the integrated current flowing to both those regions without photon input and those with photon input is measured. The difference in these quantities will be called the signal amplitude.

In terms of the equivalent circuit, consider that the circuit represents a diode or picture element. Some fraction p of a frame time prior to $t = 0$, the switch was briefly closed and the capacitor acquired the battery potential. Then at time τ the current generator furnished a unit pulse of charge. Then after time T plus an additional $(1-p)$ frame times, the switch was briefly closed again and the charge passing from the battery to charge the capacitor was measured. This constitutes a measurement of the video signal plus accumulated dark current. The experiment is also repeated, but without the current generator pulse, to measure only the accumulated

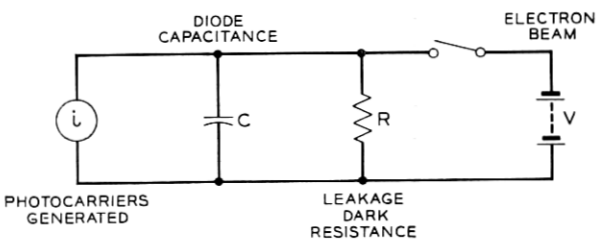

Fig. 6 — Equivalent circuit for one picture element in a diode array camera tube.

dark current. The difference of these two measurements is again the signal amplitude.

The reader may determine by a simple circuit analysis that T is varied the signal amplitude changes in proportion of $\exp(-T/RC)$. Thus by varying the frame delay time T it is possible the charge storage time $\tau_s = RC$ of the circuit.

Such an experiment was carried out with the tube just described, No. TN-84, and it was found that the signal amplitude did decay exponentially as a function of the frame delay time T. The only departure from exponential decay occurred at very long delays and was found to be caused by there being insufficient beam current available to completely charge down the target after such a long-time loss of charge. The results were that the charge storage time was 0.184 ± 0.027 seconds at 27.5°C, increasing to 1.197 ± 0.341 seconds in the range 7 to 11°C. Since this target did not have diodes with low leakage currents, showing instead the relatively large dark current of 70 nA/cm^2 at 32°C, other diode array targets should have even longer charge storage times. Charge storage times as long as $\approx$85 seconds seem to be possible with better targets (this assumes a cooled target with dark current 0.1 nA/cm^2 and a typical diode capacitance value of 2000 pF/cm^2). Storage times longer than about a minute are probably not needed in sequential imaging applications, since film is a convenient medium for such long exposure times.

The result is that for typical sequential imaging applications both the silicon diode array and potential X-ray photoconductive target materials (selenium, CdS, and PbO) have sufficiently long charge storage times to be used. The next point taken for comparison between different camera tubes will be sensitivity.

As before, camera tubes will be compared assuming blocking contacts, but only a relatively thin depletion region, so that carriers must diffuse to an electrode for collection. To compare sensitivity, it will be assumed that the photosensitive target material is chosen to have the thickness of one carrier diffusion length to insure high collection efficiency. In the case of silicon this implies a target thickness of 0.004 inch, which does lead to the very greatest sensitivity in the predicted curves of Fig. 4. For selenium this gives a target thickness of 10μ, which agrees with the optimum target thickness reported by Smith.[40] The same assumptions will be made about CdS and PbO for this comparison. Obviously the question of optimum target thickness depends upon not only the bulk and surface properties of the materials, but upon the energy of X-rays which it is desired to detect, and

the comparison here can only be qualitative. Nevertheless, it is instructive to consider how the sensitivities of various types of camera tubes would compare for use in the lower energy region such as that appropriate for crystal diffraction studies; these assumptions offer a simple and unbiased means for evaluation.

Another piece of information needed is the average energy, ΔE, required to free a carrier. Measured values are available for PbO, CdS, and silicon, but aparently not in the case of selenium. These energies typically seem to be roughly proportional to the band gap energy in the material, as shown in Table III and discussed somewhat in Ref. 57. Thus a value of ΔE for selenium is estimated that is consistent with the other values and tends to be optimistic in its predictions of sensitivity (that is, the value of ΔE is as small as would be consistent with other values in the table). The typical energies for these applications are taken to be 10 keV and 25 keV for this com-

TABLE III — COMPARISON OF CAMERA TUBES FOR LOW-ENERGY IMAGING

Substrate Material	PbO Tetragonal	Se Amorphous	CdS n-type	Si n-type
Absorption discontinuities between 5 and 30 keV*	13.03–15.86 L_{Pb}	12.65 K_{Se}	26.712 K_{Cd}	none
Target thickness t, μm(= diffusion length)†	1.2	10	6.4	110
Carrier production energy, ΔE, in eV	8‡	≈6.7§	≈8.3¶	3.5‖
Ratio of ΔE to band gap#	3.48	3.19	3.46	3.18
Absorption coef. α, $(\mu m)^{-1}$:†				
E = 10 keV	0.1117	0.0226	0.0496	0.00804
E = 25 keV	0.0465	0.0134	0.00431	0.000576
f = 1 − exp (−αt):				
E = 10 keV	0.125	0.202	0.272	0.586
E = 25 keV	0.054	0.126	0.027	0.060
Geometrical efficiency g	—	0.80**	—	0.88††
Relative response, S = fE/ΔE:				
E = 10 keV	156	302	328	1680
E = 25 keV	169	470	81	428

* *Handbook of Chemistry and Physics*, 48th ed., Chemical Rubber Company, p. E-125.

† See Table II for references.

‡ See Ref. 57.

§ Estimated to make the ratio of ΔE to band-gap the same as for silicon, which constitutes an optimistic estimate for the purpose of estimating the overall sensitivity.

¶ The average of the values 7.3 and 9.3 quoted by Lappe (Ref. 57).

‖ See Ref. 19.

Band gap energies are from R. H. Bube, *Photoconductivity of Solids*, New York: John Wiley & Sons, 1960, pp. 233–234.

** For target thickness 0.001″. See Ref. 39.

†† From Fig. 6 of this article, with t = 0.004″ and E = 10 and 25 keV.

parison, and the usable fraction of the incident photons $f = 1 - \exp(-\alpha t)$ can be calculated in terms of the absorption coefficient α and the thickness t of the target, as shown in Table III.

The relevant target parameter that determines the size of the video signal is the product ηf. Since η is the number of video electrons collected per usefully absorbed X-ray photon, and since each photon produces a number of carriers equal to $E/\Delta E$, it follows that

$$\eta = gE/\Delta E. \tag{5}$$

In this equation, g is the geometrical efficiency, the same quantity discussed in connection with Fig. 4, which was defined as the fraction of free carriers generated which lead to video current. Since the target thickness has been taken equal to the carrier diffusion length, the geometrical efficiency will be quite high, as may be determined from Fig. 4. Table III shows typical values for g for silicon and selenium. Because of the choice of target thicknesses, it is appropriate to assume that the geometrical efficiency will be close to unity for all the target materials here considered. Therefore, instead of comparing relative sensitivities on the basis of $\eta f = gfE/\Delta E$, a meaningful comparison of sensitivity can be made by simply comparing the quantity

$$S = fE/\Delta E. \tag{6}$$

Thus a comparison of sensitivity between various scanned camera tubes for low-energy imaging can be made in a semiquantitative way by comparing a single sensitivity number S at the X-ray energies of interest. This has been done in the last two lines of Table III for X-ray energies of 10 and 25 keV.

The PbO target performs poorly because of its extremely short carrier diffusion length, necessitating a very thin target. At 25 keV selenium is the most sensitive, followed closely by silicon; at 10 keV silicon is by far the most sensitive (selenium has less than 20 percent of its sensitivity). To emphasize the sensitivity of silicon, notice that X-ray imaging in the 10 keV range has been carried out with a silicon diode array with sensitivity approximately equal to that of Polaroid film (ASA 3000) using a standard cassette with internal fluorescent screen.

If it is possible to extend the depletion region to greater depths, then increased target thicknesses may be possible without loss of geometrical efficiency. In such a case the sensitivity of any of these possible camera tubes could be greatly increased. In the case of silicon

this could be done by reducing the substrate resistivity, providing that this did not also lead to increased dark current. With the other target materials this could be accomplished by fabricating effective blocking contacts which could remain blocking up to sufficiently high voltages to extend the depletion region, or by making good p-n junctions in material of low resistivity. The most progress along these lines has probably been made with PbO targets, although the published observations concerning X-ray detection with PbO camera tubes seem to be too sparse to permit detailed comparisons with the silicon camera tube.

A further point for comparison that is relevant is the uniformity of sensitivity over the energy range that it is desired to operate. For the materials discussed here, Table III shows the positions of any absorption discontinuities occurring in the range 5 to 30 keV. Since the absorption of the elements in question changes by a large factor (2 to 5) at the energies indicated, the presence of absorption discontinuities is reflected in a great difference in the sensitivity of the camera tube on either side of these energies. This can be an inconvenience, both because of the unfamiliar appearance it may give to familiar Laue diffraction patterns and because of the great variation in threshold sensitivities when X-ray flux intensities are to be measured. From this standpoint, both PbO and selenium seem undesirable for low-energy imaging. CdS is better, having only a discontinuity at 26.712 keV, but silicon is clearly the target material least contaminated with unwelcome discontinuities in absorption. In fact, silicon has no such discontinuities above 1.838 keV, which is too low in energy for open-air diffraction work anyway.

The final point for comparison was referred to as "convenience", which includes whatever practical considerations may be relevant to selection of a camera tube for particular applications. A disadvantage of silicon diode array tubes arises when very long integration times are required, since some form of target cooling must be supplied to presently produced targets to obtain integration times much longer than a second. Although tubes are now being designed incorporating internal solid-state cooling, it would still be desirable to eliminate this additional complication. Improvements in target processing will probably permit integration times as long as ten seconds, even at room temperature, when targets with lower dark current become available.

There are other respects in which the silicon diode array looks more desirable. It can withstand high temperatures without damage (at

least several hundred degrees Centigrade), whereas an amorphous selenium target tends to crystallize above 30°C.[58] Moreover, although the diode array requires some special techniques for diffusion, the resulting target is durable and can withstand the kind of high temperature bakeout that seems always to be required when producing vacuum tubes with high reliability and years of life.

Some other general advantages to scanned camera tubes are common to all the types considered here. The dc level on the television monitor can be adjusted to provide a threshold signal below which no image appears, which is useful in removing background noise from the image. The apparent magnification of the image may be varied electronically by changing the raster size. Finally, simple electronic techniques like triggering a time-delay oscilloscope at the beginning of a frame allow the video signal current to be accurately measured at any desired locations in the image.

The question of damage resulting from incident X-radiation is still open. Silicon diode array targets coated with a silicon resistive overlay show a slight increase in dark current where they have been exposed to a direct beam from an X-ray tube. No damage at all seems to occur below a certain X-ray intensity, although this qualitative judgment may not turn out to be genuine when properly measured. Finally, this damage tends to anneal out when the tube is left warmed up without incident X-rays for a few hours, although some damage can still be detected.

These descriptive features have mainly emphasized the silicon diode array camera tube since the authors have very little information on the practical aspects of the other types of X-ray camera tubes. Commercially available tubes* are of the selenium target variety; they have relatively short life and cannot withstand high temperatures. Some information is available in the literature concerning PbO tubes[21, 41] but apparently not on CdS.

VIII. CONCLUSIONS

The following are the distinguishing features of the silicon diode array camera tube as applied to X-ray imaging. This device has high sensitivity and a smooth spectral response in the range 5 to 30 keV. Electronic zooming can be used to vary picture magnification. Silicon is easy to work with and clean for vacuum tube use; good fabrication

* Westinghouse Type WX-5129 X-Ray Vidicon, Westinghouse Electric Corporation, Electronic Tube Division, Elmira, N. Y.

technology has been developed, especially locally. Silicon camera tubes can be baked out at high temperatures.

Among the less desirable features of the silicon diode array are its relatively high dark current, requiring not too high an operating temperature, and, for low-intensity detection, requiring cooling of the target. In addition, for very long charge storage times, cooling would be necessary. The silicon diode array seems to exhibit some damage at high X-ray flux rates. It requires competent photolithographic techniques to fabricate, and for certain applications (such as medical work) it seems to be less desirable than CdS.

Future lines of work will include both improvement of the device and pursuit of practical applications. Measurements will be made of the photoemission from the surfaces of silicon diode array targets that have gone through all the usual special surface processing used to lower the surface recombination velocity. Tubes will be constructed having larger sensitive areas, at least ¾ inch in diameter, by covering the silicon disk with diodes and using a beryllium or mylar window to hold the vacuum instead of the silicon itself. Thicker targets will be used to increase X-ray absorption, and attempts will be made to make fully depleted thick targets, making use of lithium drifted silicon substrates. The possibility of carrier injection from denser materials deposited on the silicon as an overlay to increase X-ray absorption will be pursued. Tubes with internal solid-state target cooling, now being assembled and developed, will be tested. In addition, tubes may be built using internal electron multiplication as well as target cooling in hopes of carrying out photon counting and pulse height discrimination of photon energy.

Practical applications to be pursued will include techniques for X-ray orientation of crystals by conventional Laue techniques and other approaches. Some preliminary results on crystal orientation, as well as some simple topographic studies of crystals using the diode array camera tube, are reported elsewhere.[4] X-ray imaging will prove useful in several health physics applications. With proper calibration of radiation dose rather than photon flux, and beam intensity profile determinations, this technique will be useful in establishing dose distributions in X-ray beams to which humans are exposed either accidentally or intentionally, as in X-ray radiotherapy. Such measurements are being made by M. M. Weiss. Use of the camera tube as a magnifying monitor in both X-ray and electron microscopy is being evaluated, the latter by Fabian Pease. Finally, the possibility of using denser target materials such as CdS will be considered for

further pursuing possible applications of the camera tube in medicine and radiography.

IX. ACKNOWLEDGMENTS

The authors are indebted to many persons who helped in essential ways in this work. The tube fabrication problems were solved and many of the measurements carried out by D. A. Brooks. K. H. Storks assisted by providing not only some essential X-ray equipment, but many enlightening suggestions and discussions. Technical conversations with E. I. Gordon, G. E. Smith, E. F. Labuda, M. H. Crowell, and B. Hakki contributed to the theoretical treatment presented here; computer programming by A. J. Chick made it possible to present the results in a very effective way. The authors are also grateful to J. V. Dalton, R. P. Hynes, and E. J. Zimany, Sr. for important contributions to the tube fabrication, to E. J. Zimany, Jr. and L. B. Hooker for assistance with technical problems, and to J. W. Harpster for discussing his work in advance of publication.

APPENDIX

Measurements of Silicon Diode Array Target Reflectivity

In Fig. 2 the measured collection efficiency of the camera tube is shown, as corrected using published values for the reflectivity of silicon.[16] The data points show a certain oscillation in magnitude as a function of wavelength. To understand this effect more fully, the reflectivity of the target was measured:

A Bausch & Lomb grating monochromator model No. 33-86-03 with 675 grooves per mm and 3-mm slits was used with a tungsten source and a Corning No. 2-64 infrared transmitting filter, the latter serving to remove second-order diffracted rays from the output beam. An aperture 2 mm in diameter as placed at the exit slit. Light from the monochromator passed through a 6.4-cm focal length lens and was reflected from a half-silvered mirror with an angle of incidence of about 45°, and the image of the 2-mm aperture was formed on the diode array target. The limiting aperture for this incident light was an 2-cm diameter aperture placed next to the lens, and the optical path length from this aperture to the target was 13 cm. Thus the incident light arrived at angles ranging up to $\tan^{-1}(1/13) = 4.41°$ with respect to the normal to the diode array target. Light reflected from the target again passed through the half-silvered mirror and

through another lens, which imaged the surface of the target on a solar cell. The diameter and placement of this lens were such that light was accepted leaving the target at any angle up to 14° with respect to the target normal. The light was chopped at 13 Hz and synchronously detected.

The reflectivity of the target was determined by comparing the 13-Hz light signal detected in the arrangement just described with the signal measured when the diode array target was replaced with a multilayer dielectric mirror. Two such mirrors, kindly loaned by L. B. Hooker, together furnished a reference reflectivity exceeding 99 percent in the wavelength range 0.85 to 1.5 microns. Care was taken not to saturate the solar cell during these measurements.

The reflectivity thus measured is plotted in Fig. 7. The data become increasingly less accurate at longer wavelengths because of the greatly reduced sensitivity of the solar cell at these wavelengths.

Fig. 7 reveals the same sort of oscillations previously observed in the collection efficiency data points of Fig. 2. Unfortunately it is not possible to correct the measured collection efficiency data using the reflectivity of Fig. 7 to verify that all the oscillations in Fig. 2 are spurious.

There are several reasons for this. First, the spectral width for the reflectivity measurement was about 100 Å, a significant fraction of the spacing between the reflectivity minima (≈700 Å), whereas the measurements of Fig. 2 were made with a considerably narrower spectral input. Second, since the oscillations presumably arise from

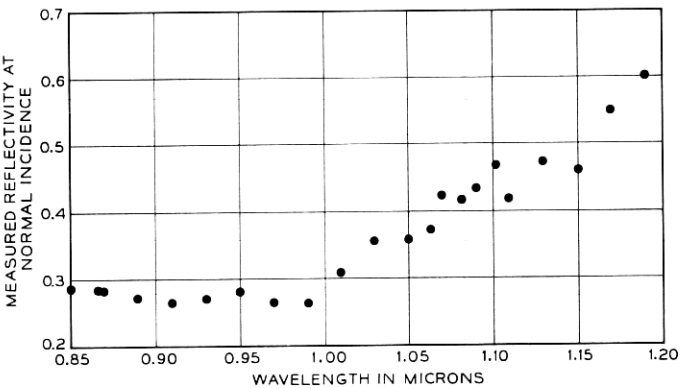

Fig. 7 — Measured reflectivity of the illuminated side of the target mounted in tube No. TN-84.

interference between multiple internal reflections in the target, their magnitudes should be strongly dependent upon the range of deviation of the incident light from the normal, which was also different in the two sets of measurements because of the different geometry used (a Perkin–Elmer monochromator was used for the collection efficiency measurements). Moreover, the collection efficiency measurements were made with the target newly mounted on the tube, but by the time the reflectivity measurements were made, the target surface had unavoidably become dirtier. These differences in surface cleanliness could easily have changed the amount of reflection either internally or externally at the silicon-air interface enough to change the magnitude of oscillations in the reflectivity from the values that would have been measured on a clean surface.

Moreover, it is not even possible to accurately compare the measured value of reflectivity (27.5 $\pm$ 1.0 percent) for wavelengths $0.80\mu\text{m} < \lambda < 1.0\mu\text{m}$ with published values of reflectivity, which amount to about 32 percent in this wavelength range.[16] It is quite possible that the scattering due to surface contamination was adequate to account for the discrepancy between the measured and the published values.

However, it is still possible to learn a lot of information from the reflectivity measurements. First they confirm the periodic behavior observed in the collection efficiency measurements. The minima in reflectivity observed at $0.91\mu\text{m}$ and $0.98\mu\text{m}$ could have arisen from interference between internal reflections in the target. Since the absorption coefficient is too great for much penetration to occur at these wavelengths, this would have to be caused by a thin surface layer of the target having slightly different optical properties from the rest of the target substrate. Its thickness may be estimated by setting

$$0.91(n + 1) = 0.98n, \tag{7}$$

from which

$$n = 13. \tag{8}$$

This gives an optical thickness for the layer of

$$\tfrac{1}{2}n(0.98) = 6.4\mu\text{m}. \tag{9}$$

Thus these oscillations in the reflectivity could be accounted for by a layer of thickness $\approx 2\mu\text{m}$ since a typical refractive index for silicon in this wavelength range is ≈ 3.6.[59] It appears that this thickness of layer would also account for the oscillation in the collection efficiency dis-

played in Fig. 2. It is not known whether such a layer could be caused by impurities or dislocations near the surface.

Since the true magnitude of the oscillation cannot be accurately known, further remarks refer to Figs. 2 and 7 with the oscillating features replaced by slowly changing average values.

As previously pointed out, the discrepancy between the measured value of reflectivity of ≈27.5 percent and the published value of 32 percent in the wavelength range 0.85–1.0μm probably results from scattering. Since the factor needed to correct the measured values of collection efficiency to obtain Fig. 2 should really be $1/T$ (T = transmission of the silicon surface for entering photons) rather than $1/(1-R)$, the measured reflectivity values should really be augmented by the scattering if they were to be used to obtain Fig. 2. Thus it seems preferable to use the larger value 32 percent, as obtained from the literature, for this correction, at least for wavelengths shorter than 1.0μm.

For wavelengths beyond 1.0μm, the published values of reflectivity continue to decrease, approaching 30 percent,[16] but the values given in Fig. 7 rise significantly at longer wavelengths. Since the absorption coefficient of the silicon decreases sharply in this wavelength range, falling to only 4.24 cm^{-1} at 1.11μm,[11] the target rapidly becomes virtually transparent to light as the wavelength increases past 1.0μm. Thus the reflectivity of the target becomes the reflectivity of the front surface, augmented by the reflectivity of the back surface (measured to be ≈40 percent by a similar technique), finally complicated at sufficiently long wavelengths by multiple internal reflection if the front and back surfaces of the target are sufficiently parallel. Thus this rise in measured reflectivity at longer wavelengths is to be expected.

REFERENCES

1. Crowell, M. H., Buck, T. M., Labuda, E. F., Dalton, J. V., and Walsh, E. J., "A Camera Tube with a Silicon Diode Array Target," B.S.T.J. *46,* No. 2 (February 1967), pp. 491–495.
2. Gordon, E. I., unpublished work.
3. Chester, Arthur N., Loomis, Thomas C., and Weiss, M. M., "Direct Imaging of Low Energy X-Rays with a Diode Array Camera Tube," Conference on Electron Device Research, Boulder, Colorado, June 19–21, 1968, (unpublished).
4. Chester, Arthur N. and Koch, Fred B., "Instantaneous Display of X-Ray Diffraction Using a Diode Array Camera Tube," 17th Annual Denver X-Ray Conference: Applications of X-Ray Analysis, Estes Park, Colorado, August 21–23, 1968, (to be published in *Advances in X-ray, Analysis,* vol. XII, Plenum Press).
5. Benson, K. E., unpublished work.
6. Evans, Robley D., "Gamma Rays," *American Institute of Physics Handbook,* ed. Dwight E. Gray, New York: McGraw-Hill, 1963, 2nd ed., pp. 8–82 and 8–95.

7. Makhov, A. F., "The Penetration of Electrons Into Solids: I. The Intensity of an Electron Beam, Transverse Paths of Electrons," Soviet Physics—Solid State, *2*, No. 9 (March 1961), pp. 1934–1941.
8. Loomis, T. C. and Weiss, M. M., unpublished work.
9. Loomis, T. C., "Statistical Precision in X-Ray Spectrochemical Analysis," to be published by General Electric Company.
10. "Table of Mass-Absorption Coefficients," Instruments Division, Philips Electronic Instruments Company, Mt. Vernon, N. Y.
11. Runyan, W. R., *Silicon Semiconductor Technology,* New York: McGraw-Hill, 1965, p. 187.
12. Chester, Arthur N., unpublished work.
13. Crowell, M. H. and Labuda, E. F., unpublished work: "The Silicon Diode Array Camera Tube."
14. Buck, T. M., Casey, H. C., Jr., Dalton, J. V., and Yamin, M., "Influence of Bulk and Surface Properties on Image Sensing Silicon Diode Arrays," B.S.T.J., *47*, No. 9 (November 1968), pp. 1827–1854.
15. Gordon, E. I. and Crowell, M. H., "A Charged Storage Target for Electron Image Sensing," B.S.T.J., *10* (December 1968), pp. 1855–1874.
16. Runyan, W. R., *Silicon Semiconductor Technology,* New York: McGraw-Hill, 1965, p. 198.
17. Labuda, E. F., unpublished work. See also McKelvey, John P., *Solid State and Semiconductor Physics,* New York: Harper and Row, 1966, p. 402.
18. Kittel, Charles, *Introduction to Solid State Physics,* New York: John Wiley and Sons, 1937, 3rd ed., pp. 308 and 323.
19. Miller, G. L., Gibson, W. M., and Donovan, P. F., "Semiconductor Particle Detectors," Ann. Rev. Nuc. Sci., *12* (1962), pp. 189–220.
20. Harpster, J. W., unpublished work.
21. Jacobs, John and Berger, Harold, "Large-Area Photoconductive X-Ray Pickup-Tube Performance," Electrical Engineering, (February 1956), pp. 158–161.
22. Teves, M. C. and Tol, T., "Electronic Intensification of Fluoroscopic Images," Philips Technical Review, *14*, No. 2 (August 1952), pp. 33–43.
23. Bertin, Eugene P., "Visual Presentation of X-Ray Diffraction Patterns by Electronic Means," Analytical Chemistry, *25*, No. 5 (May 1953), pp. 708–721.
24. Tol, T. and Oosterkamp, W. J., "The Perception of Small Object-Detail," section II of "The Application of the X-Ray Image Intensifier," Philips Technical Review, *17*, No. 3 (September 1955), pp. 71–77.
25. Feddema, J., "Medical Aspects of the Image Intensifier," section V of "The Application of the X-Ray Image Intensifier," Philips Technical Review, *17*, No. 3 (September 1955), pp. 88–93.
26. Schott, Ottfried, "Bildverstärker und Fernsehen in der Röntgen-Diagnostik," Elektrotechnische Zeitschrift, *A85*, No. 19 (September 18, 1964), pp. 606–610.
27. Wegener, Arthur F., "An X-Ray Image Intensifier of the Closed Circuit Television Type," Nondestructive Testing, (January–February 1958), pp. 16–23.
28. *International Tables for X-Ray Crystallography,* Vol. III, ed. Caroline H. MacGillavry, Gerard D. Rieck, and Kathleen Lonsdale, Birmingham, England, The Kynoch Press, 1962, Sec. 3.1, pp. 133–156.
29. Herstel, W., "The Assessment of Image Quality in Medical Fluoroscopy," in *Photo-Electronic Image Devices,* proceedings of the third symposium held at Imperial College, London, September 20–24, 1965; *Advances in Electronics and Electron Physics,* Vol. 22A, ed. L. Marton, New York: Academic Press, 1966, pp. 363–368.
30. Harpster, J. W. and Jacoby, B. F., "Radiation Imaging with Electron Beam Scanning of *p-n* Junction Diode Arrays," Abstract No. D8 in Bull. Am. Phys. Soc., *13*, No. 7 (July 1968), p. 957.
31. Hoerlin, Herman and Mueller, F. W. H., "Gold Sensitization of X-Ray Films," J. Opt. Soc. Am., *40*, No. 4 (April 1950), pp. 246–251.
32. The Commission on Crystallographic Apparatus of the International Union of Crystallography, "A Comparison of Various Commercially Available X-Ray Films," Acta Cryst., *9*, part 6 (June 10, 1956), pp. 520–525.

33. Stahnke, Ingeborg and Heinrich, Hans, "Special Problems in Measuring the Modulation Transfer Function of X-Ray Image Intensifiers," in *Photo-Electronic Image Devices,* proceedings of the third symposium held at Imperial College, London, September 20–24, 1965; *Advances in Electronics and Electron Physics,* Vol. 22A, ed. L. Marton, New York: Academic Press, 1966, pp. 355–362.
34. Guyot, L. F. and Driard, B., "X-Rays Image Intensifiers Latest Developments: 3,000 gain 6" and 9" X-Rays C.F.T.H. Tubes," Le Vide, *85,* (January–February 1960), pp. 28–35.
35. Picker Special Products Catalog, publication No. 52–21 of Picker X-Ray Corporation, White Plains, New York.
36. Pierce, J. R., *Theory and Design of Electron Beams,* D. Van Nostrand Company, Princeton, New Jersey, 1954, 2nd ed., p. 121.
37. McNair, D., unpublished work.
38. Labuda, E. F., private communication.
39. Cope, A. D. and Rose, A., "X-Ray Noise Observation Using a Photoconductive Pickup Tube," J. Appl. Phys., *25,* No. 2 (February 1954), pp. 240–242.
40. Smith, C. W., "An X-Ray Sensitive Photoconductive Pick-up Tube," in *Photo-Electronic Image Devices,* proceedings of a symposium held at London, September 3–5, 1958, Vol. XII in *Advances in Electronics and Electron Physics,* ed. by L. Marton, Academic Press, New York, 1960, pp. 345–361.
41. Heijne, L., Schagen, P., and Bruining, H., "An Experimental Photoconductive Camera Tube for Television," Philips Technical Review, *16,* No. 1 (July 1954), pp. 23–25.
42. Bichsel, Hans., "Passage of Charged Particles Through Matter," section 8c of *American Institute of Physics Handbook,* ed. Dwight E. Gray, New York: McGraw-Hill, 1963, 2nd ed., pp. 8–43.
43. Verse, H. and Jensen, H., "Equipment for Spot Film Radiography Incorporating an Image Intensifier Fitted with a Periscope Optical System," section IV of "The Application of the X-Ray Image Intensifier," Philips Technical Review, *17,* No. 3 (September 1955), pp. 84–88.
44. Garthwaite, E., "X-Ray Image Intensifiers Using Image Orthicon Tubes," in *Photo-Electronic Image Devices,* proceedings of a symposium held at London, September 3–5, 1958; *Advances in Electronics and Electron Physics,* Vol. XII, ed. L. Marton, New York: Academic Press, 1960, pp. 379–387.
45. Rose, A., "Television Pickup Tubes and the Problem of Vision," in *Advances in Electronics,* ed. by L. Marton, New York: Academic Press, 1948, pp. 131–166.
46. DeHaan, E. F., "Signal-to-Noise Ratio of Image Devices," in *Photo-Electronic Image Devices,* proceedings of a symposium held at London, September 3–5, 1958; of *Advances in Electronics and Electron Physics,* Vol. XII, ed. L. Marton, New York: Academic Press, 1960, pp. 291–306.
47. Goetze, G. W. and Taylor, A., "Direct Viewing and Rapid Photographic Recording of X-Ray Diffraction Patterns," Rev. Sci. Inst., *33,* No. 3 (March 1962), pp. 353–359.
48. Harpster, J. W. and Jacoby, B. F., "Vidicon Optical and Nuclear Radiation Imaging Employing a Silicon Mosaic Array Target," Technical Conference on the Preparation and Properties of Electronic Materials, sponsored by Metallurgical Society of the AIME, Chicago, August 12–14, 1968, (proceedings to be published as March 1969 issue of Trans. Metallurgical Soc.)
49. Rose, Albert, *Concepts in Photoconductivity and Allied Problems,* New York: John Wiley and Sons, 1963, pp. 4–10 and 131–134.
50. Rose, A., "Maximum Performance of Photoconductors," Helv. Phys. Acta, *30,* No. 4 (August 15, 1967), pp. 242–244.
51. Redington, R. W., "Maximum Performance of High-Resistivity Photoconductors," J. Appl. Phys., *29,* No. 2 (February 1958), pp. 189–193.

52. van den Broek, J., "Physical Interpretation of a PbO-Photodetector," Solid State Commun., *4,* No. 6 (June 1966), pp. 295–297.
53. Spear, W. E. and Mort, J., "Electron and Hole Transport in CdS Crystals," Proc. Phys. Soc., *81,* part 1 (January 1963), pp. 130–140.
54. Greatorex, C. A., "Image Intensification Using a Flying-Spot X-Ray Tube," in *Photo-Electronic Image Devices,* proceedings of a symposium held at London, September 3–5, 1958; *Advances in Electronics and Electron Physics,* Vol. XII, ed. L. Marton, New York: Academic Press, 1960, pp. 327–344.
55. Dozier, C. M., Gilfrich, J. V., and Birks, L. S., "Quantitative Calibration of X-Ray Film Response in the 5-keV to 1.3-MeV Region," Appl. Opt., *6,* No. 12 (December 1967), pp. 2136–2139.
56. Schottmiller, John C., "Photoconductivity in Tetragonal and Orthorhombic Lead Monoxide Layers," J. Appl. Phys., *37,* No. 9 (August 1966), pp. 3505–3510.
57. Lappe, F., "The Energy of Electron-Hole Pair Formation by X-Rays in PbO," J. Phys. Chem. Solids, *20,* Nos. 3 and 4 (August 1961), pp. 173–176.
58. Weimer, Paul K. and Cope, A. Danforth, "Photoconductivity in Amorphous Selenium," RCA Review, *12,* No. 3 (September 1951), pp. 314–334.
59. Runyan, W. R., *Silicon Semiconductor Technology,* New York: McGraw-Hill, 1965, p. 200.